Materials and Structures (2016) 49:1213–1220
DOI 10.1617/s11527-015-0571-0

ORIGINAL ARTICLE

Structural built-up of cement-based materials used for 3D-printing extrusion techniques

A. Perrot · D. Rangeard · A. Pierre

Received: 14 October 2014 / Accepted: 16 February 2015 / Published online: 24 February 2015

Abstract Additive manufacturing and digital fabrication bring new horizons to concrete and cement-based material construction. 3D printing inspired construction techniques that have recently been developed at laboratory scale for cement-based materials. This study aims to investigate the role of the structural build-up properties of cement-based materials in such a layer by layer construction technique. As construction progresses, the cement-based materials become harder with time. The mechanical strength of the cement-based materials must be sufficient to sustain the weight of the layers subsequently deposited. It follows that the comparison of the mechanical strength, which evolves with time (i.e. structural build-up), with the loading due to layers subsequently deposited, can be expected to provide the optimal rate of layer by layer construction. A theoretical framework has been developed to propose a method of optimization of the building rate, which is experimentally validated in a layer-wise built column.

Keywords Additive manufacturing · Cement-based materials · Yield stress · Structural build-up

A. Perrot (✉)
Laboratoire d'Ingénierie des MATériaux de Bretagne, (LIMATB), Université de Bretagne Sud – Université Européenne de Bretagne, Centre de Recherche de Saint-Maudé, BP 92116, 56321 Lorient, Cedex, France
e-mail: arnaud.perrot@univ-ubs.fr

D. Rangeard
Laboratoire de Génie Civil Génie Mécanique (LGCGM), Institut National des Sciences Appliquées, Université Européenne de Bretagne, 20, avenue des buttes de Coësmes, CS 14315, 35043 Rennes, Cedex, France
e-mail: damien.rangeard@insa-rennes.fr

A. Pierre
Laboratoire Mécanique et Matériaux du Génie Civil (L2MGC), Université de Cergy-Pontoise, 5 mail Gay-Lussac, Neuville sur Oise, 95031 Cergy-Pontoise, Cedex, France
e-mail: Alexandre.pierre@u-cergy.fr

1 Introduction

Additive manufacturing and digital fabrication bring new horizons to concrete and cement-based material construction. The possibility to build concrete structures without formwork is a major advantage in terms of production rate, architectural freedom and cost reduction; as noted in [1], formwork represents 35–60 % of the overall costs of concrete structures.

Moreover, it allows human labour to be replaced by digitally controlled robots and furthermore allows the implementation of these new techniques in highly polluted environments and in spatial applications [2].

Various techniques have been developed in recent years; for example, smart dynamic casting is a result of a combination of slipforming and digital fabrication techniques [1, 3]. Another family of concrete digital manufacturing has been inspired by the 3D printing

technique [4]. This technique is commonly called 'additive manufacturing' and consists of joining materials to produce objects, layer upon layer, from 3D model data. Examples of such techniques belonging to this family of digital-aided construction are the "Concrete printing" process developed at Loughborough University [5–9] and the "Contour Crafting" method [10, 11] developed at the University of Southern California.

One way of additive manufacturing in construction of concrete is to combine concrete extrusion with digital fabrication techniques. As noted in [1], the objective is a scaling-up of a desktop 3D printer to the size of a building site. At this time such techniques are not sufficiently developed for industrial application but have succeeded in producing wall elements under laboratory conditions [7, 8, 10].

Nevertheless, additive manufacturing extrusion technique can be developed into a very efficient and robust construction technique at an industrial scale. To achieve this end and optimize the process, two major constraints need to be overcome [1]: Firstly the bonding between the layers which is a weakness in the printed structure. It is worth noting that the bonding strength decreases with the time gap between layers [8]. The second constraint is the monitoring of the material hardening over time: The material must be hard enough to sustain the weight of the subsequently deposited layers. This constraint may lead to a prolonged production time.

The juxtaposition of these two constraints confronts us with a paradox concerning the production rate of this process. The time gap between two deposited layers must be sufficiently long to provide adequate mechanical strength capable of sustaining the weight of the subsequently deposited layers and also short enough to ensure both optimized bonding strength and building rate.

It therefore appears that the optimized time gap between layers should be the shortest that allows the stability of the structure during construction. Such optimized time gap brings the highest bonding strength and building rate compatible with a stable structure of deposited fresh concrete.

The ability of the deposited layers to sustain its own weight is linked to its rheology and more particularly to its yield stress [3, 7]. During the layer by layer building of a wall, the first deposited layer undergoes the heaviest load. In order to ensure the wall stability during the process, the yield stress must be sufficient to sustain this load. At this point, a new paradox appears: the paste must be sufficiently fluid for extrusion purpose [12] but sufficiently firm for the structure mechanical stability. A way around this paradox is to use the structural build-up of the concrete to ensure both, sufficient fluidity during extrusion and stability after deposit. The yield stress of cement-based materials increases over time at rest [13–19]; this reversible behaviour is due to the nucleation of cement grains at their contact point by CSH formation during the dormant period before the setting time [20]. This yield stress increase is commonly modelled using a linear relationship with resting time [15] during the first hour of rest. Recently, Perrot et al. have proposed an exponential relationship that describes the yield stress increase up to the setting time [21]. It has been shown that the structural build-up properties of cement-based materials can be used to predict or optimize concrete production. For instance, formwork pressure reduction or distinct-layer casting issues can be predicted using the structural build-up rate of self-compacting concrete [21–24]. In the present case, structural build-up is used to describe and model the competition between the load increase, linked to the building rate, and the mechanical strength of the first deposited layer of the structure which is linked to the cement-based material yield stress. The aim of this paper is to propose a model that predicts the structure failure (or stability) during the additive manufacturing process of a concrete structure. This model is potentially a tool for optimizing the building rate of concrete in 3D printing.

In the first part of the paper, a theoretical framework is developed for structural build-up of cement-based materials and load due to 3D printing is proposed. Experimental tests are then carried out on a firm paste to simulate the loading due to the printing of a concrete column. Finally, the comparison between both the theoretical framework and the experimental results highlights the finding that structural build-up must be taken into account in additive manufacturing extrusion technique in order to find the highest acceptable building rate.

2 Theoretical framework

Many studies on digital fabrication techniques have shown that the building rate of the structure influences

the success of the process [1, 3, 7]. For additive manufacturing exturion technique, Le et al. [7] defines an open time (linked to the Vicat setting time), to describe the change of the concrete workability with time. This parameter is likely to affect what the authors called "buildability," which consists of quantifying the number of filament layers that could be built up without noticeable deformation of lower layers.

The idea of this theoretical framework is to compare the mechanical strength of the bottom first deposited layer with the mechanical load due to the weight of the above-deposited layers, and then to model the so-called "buildability" defined in [7]. It is then necessary to model both the evolution of the mechanical strength of the cement-based material before hydration (which is governed by the material yield stress) and the evolution in time of the mechanical load due to the building of the structure. The developed theory must be able to indicate if the layered structure is able to sustain its own weight and able to predict the failure time when the structure is going to collapse.

In case of a wall or a column construction, the vertical stress acting on the first deposited layer increases in time with the built height of the structure. Even if the vertical stress increases step by step as new layers are deposited, an average rate of construction can be computed over the construction time. Initially, it would appear natural to choose a constant rate of vertical construction. This rate of construction is designated by R.

Then, the vertical stress σ_v acting on the first layer can be written as follows:

$$\sigma_V = \rho g h(t) = \rho g R t \quad (1)$$

where ρ is the specific weight of the concrete, t is the age of the first deposited layer (which starts with its deposition) and h is the height of the vertical structure located above the first deposited layer.

The stability of the first layer can be tested by comparing the vertical stress given by Eq. (1) with a critic failure stress, which is linearly linked to the yield stress of the first deposited material:

$$\sigma_c(t) = \alpha_{geom}.\tau_0(t) \quad (2)$$

where $\tau_{0,0}$ is the yield stress of the first deposited material and α_{geom} is a geometric factor which depends of the form of the built structure.

The increase in yield stress is commonly considered to be linear during the dormant period prior to setting [13, 14]. Roussel [14, 15] has defined the structuration rate A_{thix} as the constant rate of increase in yield stress over the time at rest:

$$\tau_0(t) = \tau_{0,0} + A_{thix} t \quad (3)$$

where $\tau_{0,0}$ is the yield stress of the material with no time at rest.

The concrete structural build-up is due to complex and coupled phenomena: flocculation due to colloidal interactions and CSH nucleation at the contact points between cement grains [16, 20]. According to Roussel et al. [20], the flocculation process lasts only several tenths of seconds. After flocculation, at a timescale of several tenths of minutes, the structural build-up is due to the formation of CSH bridges between cement grains at the pseudo contact-points. The authors assumed that the rate of formation of CSH bridges is constant because the heat of hydration is constant during the so-called "dormant" period. Therefore, they conclude that, during this period, the increase of yield stress with time (or the elastic modulus) must be linear.

After this linear increase period which lasts up to 60 min, the rate of yield stress increase speeds up [21, 25, 26]. It would therefore appear that there is a non-negligible linear increase of the solid volume fraction which leads to an exponential increase in yield stress.

Perrot et al. [17] have proposed an exponential yield stress evolution that describes a smooth transition from the initial linear increase to the exponential evolution and asymptotically tends to the Roussel model as t_t tends to zero:

$$\tau_0(t) = A_{thix} t_c \left(e^{t_{rest}/t_c} - 1 \right) + \tau_{0,0} \quad (4)$$

where t_c is a characteristic time, the value of which is adjusted to obtain the best fit with experimental values.

The geometric parameter α_{geom} depends on the form of the built structure. In a straight vertical construction, the horizontal cross section and the height of a deposited layer are the parameters that are used to compute α_{geom}. For example, for circular column of diameter D, α_{geom} can be computed from the theory of squeeze flow of plastic material [27, 28]. To make an analogy between squeeze flow and 3D printing extrusion technique, it can be considered that

the first deposited layer is confined between two plates, the ground and the bottom surface of the layer deposited above. In this first approach, the surfaces of these two plates are assumed to be rough in order to comply with the adherent hypothesis for the wall conditions. Thus, using the expression given in [27, 28], the α_{geom} parameter can be expressed as:

$$\alpha_{geom} = 2\left(1 + \frac{D}{2\sqrt{3}h}\right) \quad (5)$$

It should be noted that other form of α_{geom} parameters are required for other types of construction such as a wall. They can be found by a static analysis or by empirical fitting.

It is worth noting that the viscous behaviour of concrete is neglected because this study focuses on the onset of flow i.e. at zero shear rate. In this first approach, we choose to neglect the weight of the first deposited layer.

3 Materials and methods

To validate our theory, we simulate the load acting on a cylindrical sample (i.e. the first deposited layer) due to the layer by layer construction of a cylindrical column. The cylindrical sample was 35 mm high and has a diameter of 60 mm. The initial material yield stress was 4 kPa and was sufficient to provide adequate strength to overcome the gravitational effect; consequently, the fresh sample could sustain its own weight. The material yield stress was higher than those found in studies carried out at Loughborough University [5–9] (which were of the order of 1 kPa) but appeared to be in the range of material yield stress used for contour crafting [10, 11] developed in University of Southern California.

To achieve this yield stress value, cement paste containing cement, kaolin and limestone filler were used. The dry binder content, expressed as a weight, was 50 % cement, 25 % limestone filler and 25 % kaolin. The water/cement mass ratio was 0.41 and a polycarboxylate-type polymer powder SP was added to the mix (SP/cement mass ratio being 0.3 %).

In this study a CEM I type cement of 3.15 specific density was used. The specific surface area of the cement, measured using a Blaine apparatus, was 3390 cm^2/g with an average particle size of 10 μm. The kaolin clay used was a Powdered Polwhite BB from Imerys® (Kaolins de Bretagne, Ploemeur, France). The specific gravity of the clay was 2.65, the largest clay grain size approximately 40 μm and mean grain size close to 9 μm. The Limestone filler had a particle size distribution ranging from 0.1 to 100 μm (d_{50} = 15 μm).

The mixes were prepared by mixing the dry powder constituents together for 2 min at 60 rpm and water was then mixed with cement in a planetary Hobart mixer. The mixing phase consisted of two steps: 2 min at 140 rpm and 3 min at 280 rpm.

In order to simulate the loading to layer by layer construction, the sample which corresponded to the first deposited layer, was placed between two parallel plates. The upper plate was then loaded in 1.5 N increments. The time gap between each loading increment allowed monitoring of the average building rate. Time gap ranging from 11 to 60 s allows the simulation of column 3D printing with an average building rate ranging from 1.1 to 6 $m.h^{-1}$. When the critical stress is exceeded, the sample could be expected to Plastically deform. To detect this plastic failure, the upper plate displacement was recorded with respect to time using a LVDT-type displacement transducer; simultaneously, fractures onset at the surface of the sample is monitored during the test. Each time gap was tested at least twice to check the test repeatability.

After mixing, measurements were carried out over a 90 min period. In this way, the evolution of the yield stress of the cement-based material with respect to time at rest was characterised as described by Perrot et al. [29]. This method is similar to the undisturbed vane test measurement presented in Khayat et al. [30]. In this study, stress growth measurements were performed approximately every 10 min at a constant shear rate of 0.001 s^{-1} as described by Mahaut et al. [31]. All samples were left at rest from the end of mixing.

Yield stress was measured using an Anton Paar Rheolab QC rheometer equipped with suitable vane geometry. After 1 min of pre-shearing, a strain growth was applied to the sample at a shear rate of 0.001 s^{-1} for 180 s. At such a low shear rate, viscous effects are negligible and yield stress can be calculated from the measured peak torque value at flow onset. The vane geometry used in this study consisted of four blades around a cylindrical shaft. For each measurement, a blade, 8 mm high and 8 mm diameter, was used. At the end of the yield stress measurement, the vane was

removed from the sample and cleaned in order to perform another measurement of sample taken from the same batch that had been previously put into another container after mixing.

For the studied material, the evolution of the yield stress with time at rest is shown on Fig. 1. Perrot et al. and Roussel models [15, 21] are also plotted on Fig. 1.

Figure 1 clearly shows that the yield stress evolution, of the tested cement paste, with time can be considered as linear during the first 40 min. It follows that the Roussel linear model [15] can be used to describe the yield stress evolution for construction process lasting less than this critical time. For longer processing, the Perrot et al. model better describes the yield stress increase [21].

4 Results and discussions

The first issue to be discussed relates to sample failure detection. The combination of monitoring fracture onset with the recording of upper plate displacement provides collaborating evidence of sample plastification. Figure 2 shows the recorded displacement of the upper plate for time gap between each layer deposit of 11, 17, 22 and 34 s. For each time gap, the moment when fractures appear on the sample surface is reported (as shown in Fig. 3). It is considered that sample failure is reached when both phenomena have occurred: fracture onset at the surface and increase in the displacement rate.

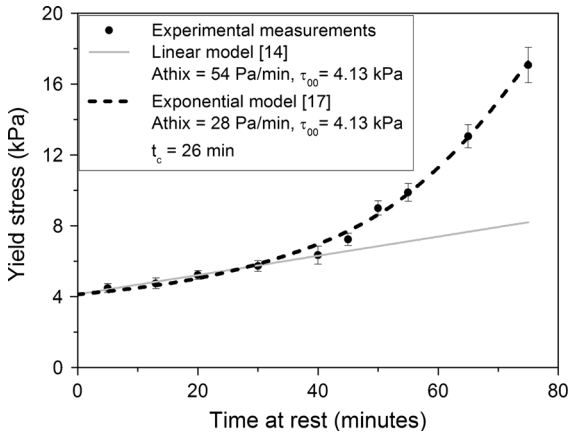

Fig. 1 Yield stress evolution with time. Comparison of the experimental results with a curve fit to the Perrot et al. [21] and Roussel models [15]

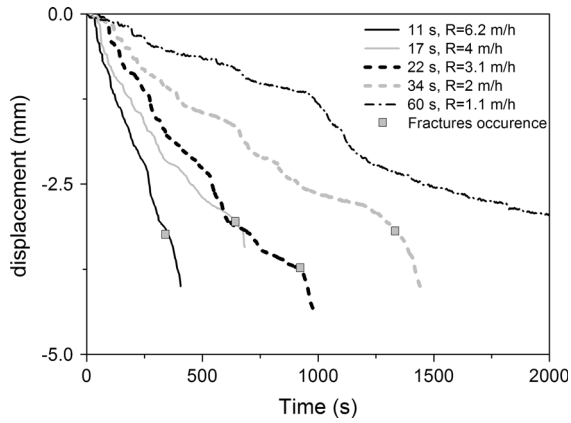

Fig. 2 Displacement of the upper plate versus time. The *grey squares* indicate the instant when fractures are observed on the surface of the samples for time gap ranging from 11 to 60 s

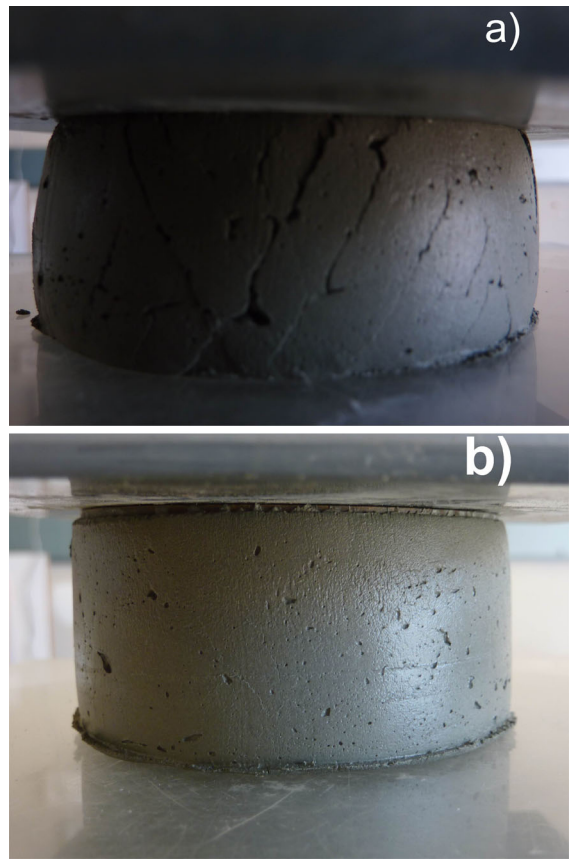

Fig. 3 **a** Fracture occurrence for a test carried out with a time gap of 17 s, **b** a sample without fractures after the test carried out with a time gap of 60 s

This detection of failure is supported by squeeze flow of semi-solid paste which undergoes fracture at the sample periphery [27, 28, 32, 33]. It can be seen in

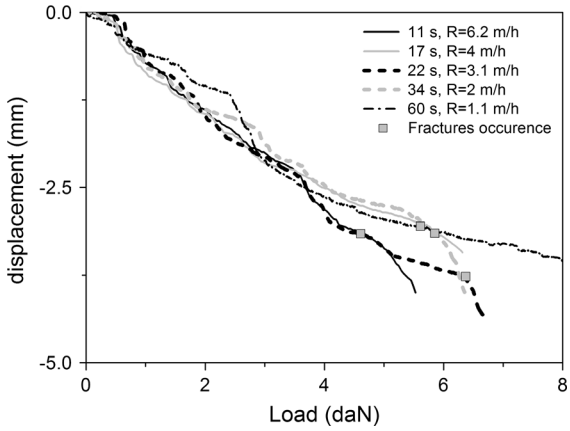

Fig. 4 Displacement of the upper plate applied load for time gap ranging from 11 to 60 s

Fig. 2 that the increase of the slope of the displacement curves occurs quasi-simultaneously with fracture occurrence.

It is also worth noting that before the change of slope and fracture onset, the displacement versus load curves are almost superimposed (Fig. 4). This superimposition provides additional evidence that before the change of slope, the behaviour of the sample is elastic and therefore no plastic flow has occurred.

Finally, we have chosen the fracture onset time as a failure indicator because it always occurred simultaneously with a change of the slope of the displacement, time curve.

All tests are summarized in Table 1 with the estimated failure times.

As expected, Table 1 shows that the building rate monitors the stability of the structure. The only sample that remains intact after the test is obtained for the smallest building rate $R = 1.1$ m/h. For higher building rate, all samples collapsed because of insufficient mechanical strength. In such cases, the material has not had time to become sufficiently stiff to sustain the weight of above deposited layers.

To go a step further, it would be interesting to predict the failure occurrence and time. As proposed in the theoretical framework, the comparison of the vertical stress with the critical stress, which is linked to the material strength, is expected to lead to a failure prediction. By plotting the evolution of both the vertical stress and the critical stress with time, as shown in Fig. 5, the time when the sample is going to plastically deform is easily identified. In this figure, the predicted time of failure is given by the intersection of the evolution of the vertical stress with the evolution of the critical stress. It is worth noting that the predicted failure time is in agreement with the experimentally observed failure time which is shown as solid circles in Fig. 5. Moreover, Fig. 5 shows that the critical stress is always higher than the vertical stress for a building rate of 1.1 m/h. This is in agreement with the experimental result which shows that the sample sustains the loading for this value of building rate. It therefore appears that the proposed theoretical framework is able to predict the success of the layerwise process of additive manufacturing. The framework provides an efficient tool to determine and optimise the building rate and therefore the bond strength between layers with the assurance of the structure stability.

It is of interest to see if an analytical prediction of the failure can be made. Using the linear evolution of the yield stress provided by Roussel [15], a critical failure time t_f can be easily expressed as follows:

$$t_{\mathrm{f}} = \frac{\tau_{0,0}}{\rho \mathrm{gR}/\alpha_{\mathrm{geom}} - A_{\mathrm{thix}}} \tag{6}$$

Table 1 Recap of all failure times and stresses

	Time gap				
	11 s $R = 6.2$ m/h	17 s $R = 4$ m/h	22 s $R = 3.1$ m/h	34 s $R = 2$ m/h	60 s $R = 1.1$ m/h
Failure time and stress	420 s 4.71 kPa	730 s 5.31 kPa	950 5.34 kPa	1320 4.80 kPa	No failure
	370 s 4.15 kPa	600 s 4.36 kPa	780 4.38 kPa	1540 5.60 kPa	
		640 s 4.65 kPa			
		655 s 4.76 kPa			
Average failure time and stress	395 s 4.45 kPa	656 s 4.76 kPa	865 4.86 kPa	1430 5.20 kPa	
SD	–	54 s 0.38 kPa	–	–	

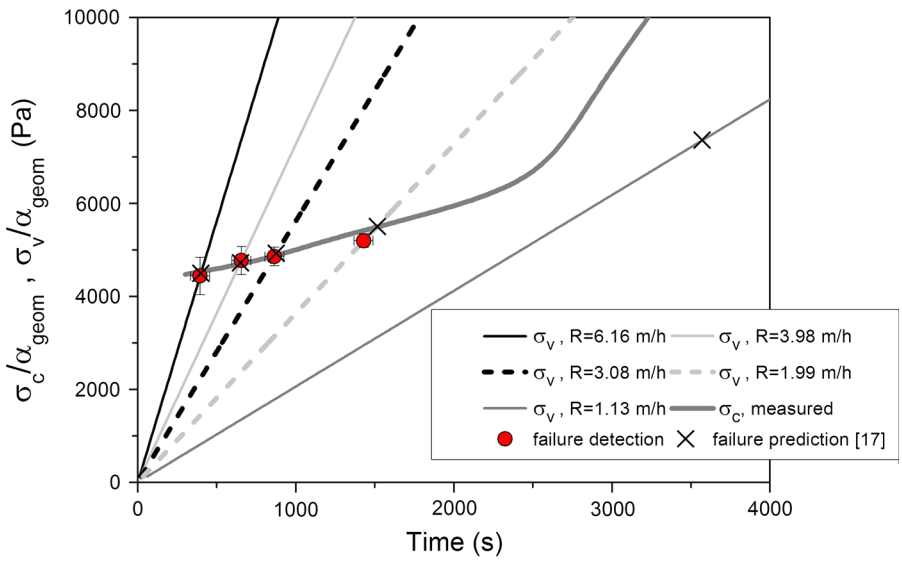

Fig. 5 Comparison of the evolution of critical stress σ_c and vertical stress σ_v for building rate ranging from 1.1 to 6.2 m/h. The *solid circles* indicate the experimental failure time and the *diagonal crosses* indicate failure time derived from a linear evolution of the yield stress

The computed failure time t_f is shown on Fig. 5 by diagonal crosses. It can be seen that the t_f values are in agreement with experimental results except for those with the smallest building rates. This discrepancy in failure time is due to the fact that for the smallest building rate, the linear description of the yield stress evolution is no longer valid for process time higher than 1500 s (i.e. 25 min). Equation (6) is valid only for failure time lower than the critical time t_c, which is given by Eq. (4) and predicts the time at which the linear model becomes inaccurate. If t_f, calculated by Eq. (6), is greater than t_c, the plot of the evolution of σ_v and σ_c with respect to time remains an effective solution to check structure stability. Furthermore, if the computed value of t_f is of the order of the setting time of the concrete, the structure is expected to remains stable during additive manufacturing extrusion technique.

5 Conclusions

In this study we have proposed a theoretical framework to find the highest building rate for layerwise concrete additive manufacturing extrusion technique inspired by 3D printing technologies. This theoretical framework is based on the comparison of the vertical stress acting on the first deposited layer with the critical stress related to plastic deformation that is linked to the material yield stress. Both stresses are time-dependent: the vertical stress depends on the building rate while the critical stress depends on the structural build-up of the concrete at rest. The developed framework consists of ensuring that the vertical stress does not exceed the critical stress.

The theoretical framework is validated by simulating the loading due to the additive manufacturing of a 70 mm diameter column. The predicted failure times of the sample are in agreement with the experimentally observed ones for all tested building rates (ranging from 1.1 to 6.2 m/h).

References

1. Lloret E, Shahab AR, Linus M, Flatt RJ, Gramazio F, Kohler M, Langenberg S (2015) Complex concrete structures: merging existing casting techniques with digital fabrication. Comput-Aided Des 60:40–49
2. Cesaretti G, Dini E, De Kestelier X, Colla V, Pambaguian L (2014) Building components for an outpost on the lunar soil by means of a novel 3D printing technology. Acta Astronaut 93:430–450
3. Shahab AR, Lloret E, Fischer P, Gramazio F, Kohler M, Flatt RJ (2013) Smart dynamic casting or how to exploit the liquid to solid transition in cementitious materials. In: Proceedings CD od the 1st international conference on rheology and processing of construction materials and of the 7th international conference on self-compacting concrete, Paris

4. Pegna J (1997) Exploratory investigation of solid freeform construction. Autom Constr 5:427–437
5. Buswell RA, Soar RC, Gibb AGF, Thorpe A (2007) Free-form construction: mega-scale rapid manufacturing for construction. Autom Constr 16:224–231
6. Buswell RA, Thorpe A, Soar RC, Gibb AGF (2008) Design, data and process issues for mega-scale rapid manufacturing machines used for construction. Autom Constr 17:923–929
7. Le TT, Austin SA, Lim S, Buswell RA, Gibb AGF, Thorpe T (2012) Mix design and fresh properties for high-performance printing concrete. Mater Struct 45:1221–1232
8. Le TT, Austin SA, Lim S, Buswell RA, Law R, Gibb AGF, Thorpe T (2012) Hardened properties of high-performance printing concrete. Cem Concr Res 42:558–566
9. Lim S, Buswell RA, Le TT, Austin SA, Gibb AGF, Thorpe T (2012) Developments in construction-scale additive manufacturing processes. Autom Constr 21:262–268
10. Koshnevis B, Hwang D, Yao KT, Yeh Z (2006) Mega-scale fabrication by contour crafting. Int J Ind Syst Eng 1:301–320
11. Zhang J, Khoshnevis B (2013) Optimal machine operation planning for construction by contour crafting. Autom Constr 29:50–67
12. Perrot A, Mélinge Y, Rangeard D, Micaelli F, Estellé P, Lanos C (2012) Use of ram extruder as a combined rheotribometer to study the behaviour of high yield stress fluids at low strain rate. Rheol Acta 51:743–754
13. Josserand L, Coussy O, de Larrard F (2006) Bleeding of concrete as an ageing consolidation process. Cem Concr Res 36:1603–1608
14. Roussel N (2005) Steady and transient flow behaviour of fresh cement pastes. Cem Concr Res 35:1656–1664
15. Roussel N (2006) A thixotropy model for fresh fluid concretes: theory, validation and applications. Cem Concr Res 36:1797–1806
16. Wallevik JE (2009) Rheological properties of cement paste: thixotropic behavior and structural breakdown. Cem Concr Res 39:14–29
17. Billberg PH (2003) Form pressure generated by self-compacting concrete. In: 3rd International RILEM symposium on self-compacting concrete, Reykjavik, Island, pp. 271–280
18. Lowke D, Kränkel T, Ghelen C, Schiessl P (2010) Effect of cement type and superplasticizer adsorption on static yield stress, thixotropy and segregation resistance. In: Khayat K, Feys D (eds) Design, production and placement of self-consolidating concrete. Springer, Heidelberg
19. Ferron RP, Greogori A, Sun Z, Shah SP (2007) Rheological method to evaluate structural buildup in self-consolidating concrete cement pastes. ACI Mater J 104:242–250
20. Roussel N, Ovarlez G, Garrault S, Brumaud C (2012) The origins of thixotropy of fresh cement pastes. Cem Concr Res 42:148–157
21. Perrot A, Pierre A, Vitaloni S, Picandet V (2014) Prediction of lateral form pressure exerted by concrete at low casting rates. Mater Struct. doi:10.1617/s11527-014-0313-8
22. Billberg PH, Roussel N, Amziane S, Beitzel M, Charitou G, Freund B, Gardner JN, Grampeix G, Graubner C-A, Keller L, Khayat KH, Lange DA, Omran AF, Perrot A, Proske T, Quattrociocchi R, Vanhove Y (2014) Field validation of models for predicting lateral form pressure exerted by SCC. Cem Concr Compos 54:70–79
23. Ovarlez G, Roussel N (2006) A physical model for the prediction of lateral stress exerted by self-compacting concrete on formwork. Mater Struct 39:269–279
24. Roussel N, Cussigh F (2008) Distinct-layer casting of SCC: the mechanical consequences of thixotropy. Cem Concr Res 38:624–632
25. Lootens D, Jousset P, Martinie L, Roussel N, Flatt RJ (2009) Yield stress during setting of cement pastes from penetration tests. Cem Concr Res 39:401–408
26. Subramaniam KV, Wang X (2010) An investigation of microstructure evolution in cement paste through setting using ultrasonic and rheological measurements. Cem Concr Res 40:33–44
27. Roussel N, Lanos C (2003) Plastic fluid flow parameters identification using a simple squeezing test. Appl Rheol 13:132–141
28. Engmann J, Servais C, Burbidge AS (2005) Squeeze flow theory and applications to rheometry: a review. J Non-Newton Fluid Mech 132:1–27
29. Perrot A, Lecompte T, Estellé P, Amziane S (2013) Structural build-up of rigid fiber reinforced cement-based materials. Mater Struct 46(9):1561–1568
30. Khayat KH, Omran AF, Naji S, Billberg P, Yahia A (2012) Field-oriented test methods to evaluate structural build-up at rest of flowable mortar and concrete. Mater Struct 45:1547–1564
31. Mahaut F, Mokeddem S, Chateau X, Roussel N, Ovarlez G (2008) Effect of coarse particle volume fraction on the yield stress and thixotropy of cementitious materials. Cem Concr Res 38:1276–1285
32. Estellé P, Lanos C, Perrot A, Servais C (2006) Slipping zone location in squeeze flow. Rheol Acta 45:444–448
33. Toutou Z, Roussel N, Lanos C (2005) The squeezing test: a tool to identify firm cement-based material's rheological behaviour and evaluate their extrusion ability. Cem Concr Res 35:1891–1899